Modeling dynamics of ECT-2/Rho/Myosin polarity circuit

Ondrej Maxian

February 15, 2024

1 The centrosome cue

The contractility circuit is forced by a cue from the centrosomes which contain Aurora A (AIR-1), an inhibitor of ECT-2. We assume that the AIR-1 signal gets to the membrane by diffusion. Letting $a(\boldsymbol{x})$ be the concentration of AIR-1 in the embryo, we have the equation

$$\Delta a = -f \qquad \boldsymbol{x} \in \Omega \tag{1a}$$

$$\nabla a \cdot \boldsymbol{n} = 0 \quad \boldsymbol{x} \in \partial\Omega, \tag{1b}$$

where (1a) is the diffusion equation for the concentration and (1b) is a no-flux boundary condition through the boundary (here Ω represents the embryo area and $\partial\Omega$ represents the boundary). The signal $f(\boldsymbol{x})$ comes from the two centrosomes, which we model by Gaussian densities

$$f(\boldsymbol{x}) = \frac{C_0}{2\pi\sigma_c^2}\sum_{i=1}^{2}\exp\left(\frac{-\|\boldsymbol{x}-\boldsymbol{x}_i\|^2}{2\sigma_c^2}\right). \tag{1c}$$

Here $\boldsymbol{x}_i$ is the location of the ith centrosome (typically at some location $(x_i, 0)$), which changes depending on the embryo conditions. In addition to the centrosome location, the signal has two other parameters: C_0, is the strength of the cue (the integral of $f(\boldsymbol{x})$ over the entire embryo cross-section; this is arbitrary and set to 1), and σ_c is the centrosome "size" (the standard deviation of the Gaussian, which is roughly half the size of the centrosome). For cytokinesis, the centrosomes have size about 2 μm, so we set $\sigma_c = 1$ μm. The solution of (1a) is unique up to a constant; we normalize all solutions so that embryos treated with PAR-3 (RNAi), where the each centrosome sits about 15 μm from its respective cortex, have an AIR-1 concentration $a(\boldsymbol{x}) = 1$ at the posterior and anterior poles

We use a standard first-order finite element method to solve (1a). In brief, the elliptical domain of the embryo is meshed into nodes and triangles, which define a set of linear Lagrangian basis

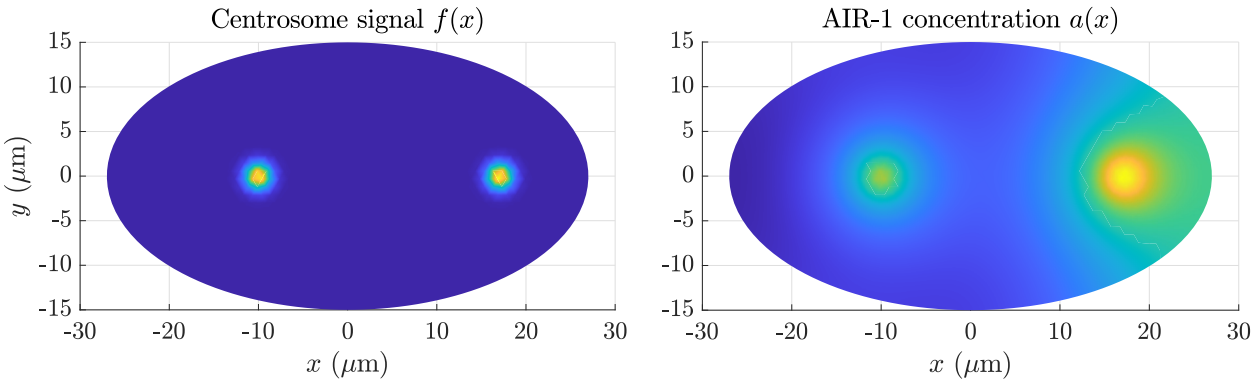

Figure 1: Solution for the diffusion equation (1) for wild-type embryos. The left panel shows the centrosome signal $f(\boldsymbol{x})$, with the anterior centrosome 17 μm away from the anterior cortex and the posterior centrosome 10 μm away from the posterior cortex. The Gaussian width $\sigma_c = 1$ (so that the centrosome diameter is roughly 2 μm). The right panel shows the solution for the concentration profile $a(\boldsymbol{x})$.

functions ψ_k that are 1 at node $\boldsymbol{x}_k$ and 0 everywhere else. Multiplying (1a) by a basis function ψ_k, then integrating by parts using the boundary condition (1b) gives

$$\sum_j \int_\Omega (\nabla\psi_k \cdot \nabla\psi_j)\, a_j \, d\boldsymbol{x} = \sum_j \int_\Omega \psi_k \psi_j f_j \, d\boldsymbol{x}, \tag{2}$$

which can be written as the matrix equation $\boldsymbol{K}\boldsymbol{a} = \boldsymbol{M}\boldsymbol{f}$, where $\boldsymbol{M}$ is the so-called mass matrix and $\boldsymbol{K}$ the stiffness matrix for finite elements. Solving $\boldsymbol{a} = \boldsymbol{K}^\dagger \boldsymbol{M}\boldsymbol{f}$ gives the solution for the concentration.

Figure 1 shows the solution of the diffusion equation over the embryo cross-section in wild-type embryos. In this case, the anterior centrosome sits 17 μm from the anterior pole, while the posterior centrosome sits 10 μm from the posterior pole. The left panel shows the AIR-1 signal, which essentially shows the location of the two centrosomes. The right panel then shows the solution to the diffusion equation (1) in this case. As might be expected, there is substantially more AIR-1 on the anterior cortex, since the centrosome sits closer to the boundary there.

We now consider how moving the centrosomes changes the profile of AIR-1 on the boundary. We use six representative treatments from [1], which modify the positions of the centrosomes. For example, in dhc-1 (RNAi) embryos, the posterior centrosome sits 3 μm from the posterior pole, while the anterior centrosome sits 45 μm from the anterior pole (9 μm from the posterior pole). As a result, the AIR-1 profile is strongly peaked at the posterior, with about 5 times the concentration there relative to the anterior. The treatments we consider can also flatten the AIR-1 profile relative

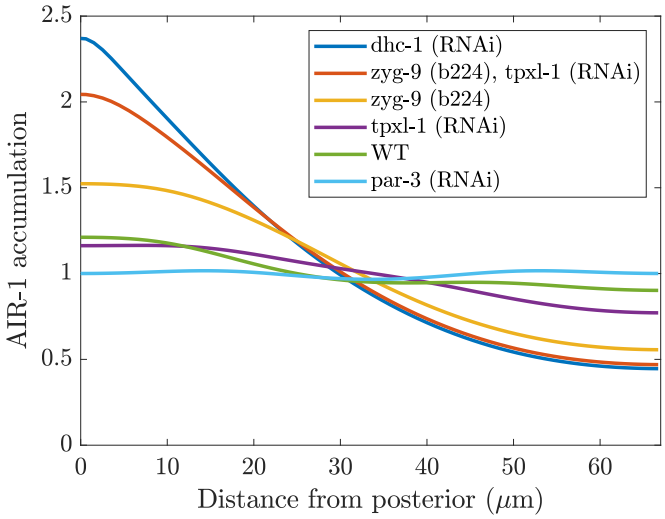

Figure 2: AIR-1 accumulation on the embryo perimeter (cortex) as predicted by the diffusion model (1). We show the AIR-1 profile as a function of distance from the posterior pole (0 is the posterior pole, 67 is the anterior pole), for embryos with six different treatments. The treatment sets the location of the centrosomes (see Fig. 3).

to wild-type, as in PAR-3 (RNAi) embryos, which have centrosomes sitting roughly at 15 μm from each pole. The profile of AIR-1 there is consequently roughly constant.

1.1 The ECT-2 response

Let us now examine how the strength of the AIR-1 signal affects the strength of the ECT-2 concentration on the proximal cortex. To do so, let us suppose that ECT-2 locally binds and unbinds from the cortex, so that the steady state dynamics obey the equation

$$k_E^{\text{on}} = k_E^{\text{off}} \left(1 + K_{\text{AE}} A\right) E \rightarrow E = \frac{k_E^{\text{on}}/k_E^{\text{off}}}{\left(1 + K_{\text{AE}} A\right)} \tag{3}$$

where K_{AE} is the strength of AIR-1/ECT-2 inhibition. In order to match the experimental data, we always normalize concentration so that $E = 1.5$ (on both the posterior and anterior cortex) in PAR-3 (RNAi) embryos. This leaves a single parameter: K_{AE}, which we tune to match the extreme dhc-1 (RNAi) embryos ($K_{\text{AE}} = 2$ gives the best fit). Figure 3 compares the resulting output (right panel) to the experimental data (left panel). While we can generally reproduce the trends observed experimental, the shape of our curve appears to be more of a line, while the experimental data show an S-shaped trend. Indeed, while we correctly predict the ECT-2 accumulation for the "extreme" embryos (dhc-1 (RNAi) and zyg-9 (b224)/tpxl-1(RNAi)), the intermediate embryos have A/P ECT-

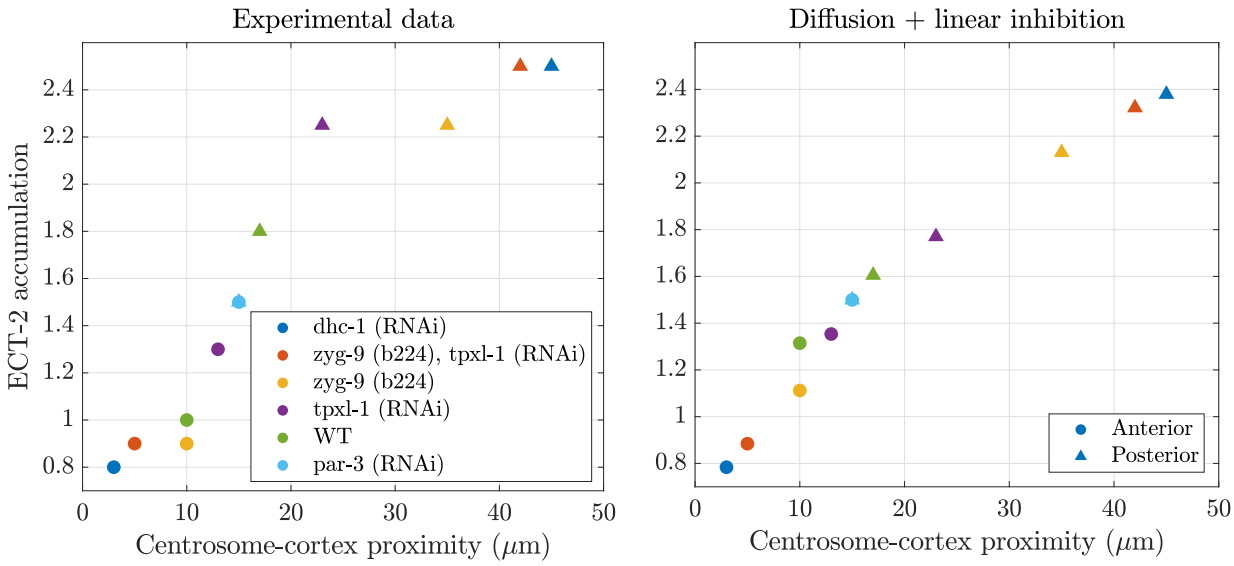

Figure 3: Comparing model results to experimental data for embryos with varying treatments (see legend at left). The left plot is a reproduction of [1, Fig. 7A], with some of the redundant embryo treatments deleted for clarity (we reduce multiple replicates to a single symbol by taking a rough average). The right plot shows the results when we consider diffusion of AIR-1 to the cortex, plus linear inhibition of the form (3), with $K_{\mathrm{AE}} = 2$.

2 disparities which are smaller than the experimental data. For example, in wild-type embryos, the experiments show an accumulation of 1.8 on the posterior, and 1 on the anterior, while our results show an accumulation of 1.6 on the posterior and 1.3 on the anterior.

Because we chose $K_{\mathrm{AE}} = 2$ to match the extreme embryos, their values are correct by design. If, by contrast, we had chosen a larger K_{AE} to match wild-type embryos, then the model results would be reversed: the wild-type embryos would be correct by design, while the extreme embryos would have A/P ratios which are much *larger* than the experiments. It seems clear that our model is missing a mechanism whereby either:

1. Small changes in ECT-2 concentration induced by diffusion (in an intermediate range) are amplified to become larger.

2. Large changes in ECT-2 concentration induced by diffusion are damped to become smaller.

Since we have not accounted for the resulting actomyosin flows which tend to concentrate ECT-2, we speculate that the first of these options is what is missing from the model. We proceed to study it next.

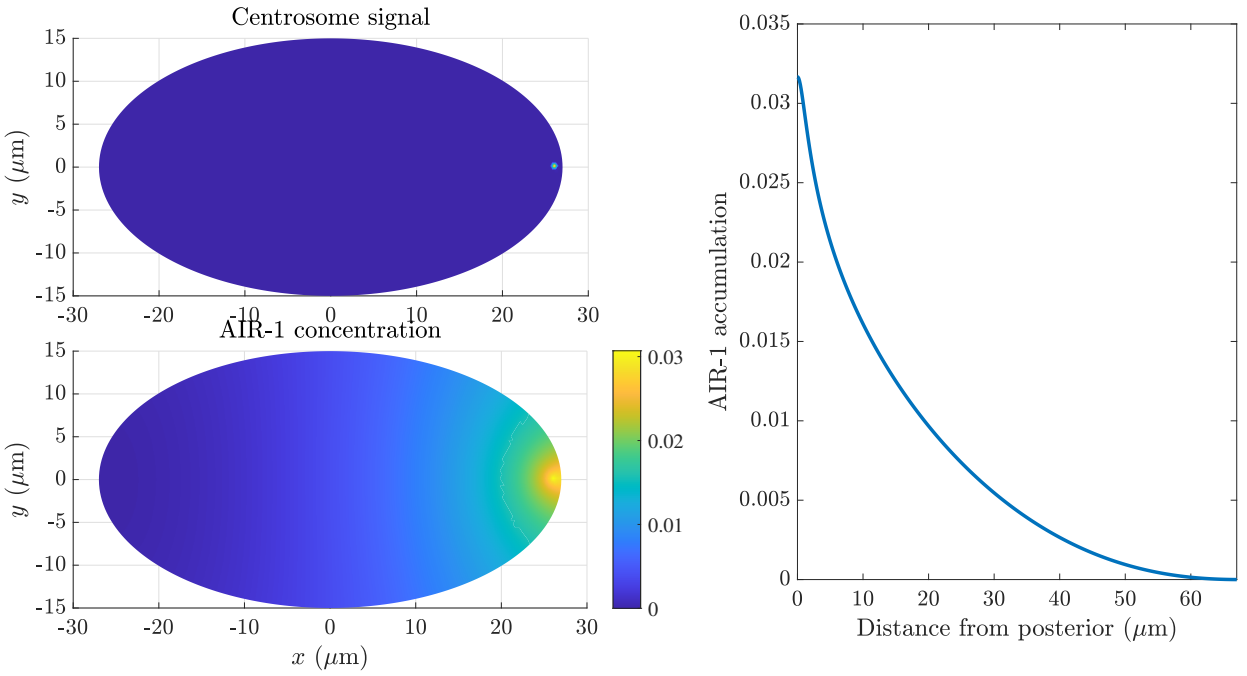

Figure 4: AIR-1 signal during polarization. In polarization, both centrosomes sit on the posterior cortex (we assume 1 μm away), have smaller size (about 0.2 μm, so we set $\sigma_c = 0.1$ μm), and contain less ($C_0 = 0.01$) AIR-1 than in cytokinesis (see plot at top left). The resulting concentration profile is shown across the entire embryo (bottom left) and along the embryo boundary (right).

1.2 Polarization model

Prior to looking at amplification of the ECT-2 signal, it is useful to also consider the dynamics during cell polarization. In cell polarization, *both* centrosomes sit on the posterior cortex (we assume 1 μm away). The centrosomes have a smaller size (about 0.2 μm, so we set $\sigma_c = 0.1$ μm). They also contain substantially less total AIR-1; here we assume that the amount scales with the area, so that $C_0 = 0.01$ for polarization. Figure 4 shows the resulting AIR-1 concentration profile across the embryo (normalized to be 0 at the posterior pole), and along the boundary. We observe a change in AIR-1 of only 0.03 from one side of the embryo to the other, which is substantially *smaller* than what we observed in cytokinesis. Considering that ECT-2 becomes asymmetrically enriched during polarization, this underscores the need to have a mechanism to amplify the asymmetries. That said, the mechanism has to work much more strongly in polarization than in cytokinesis, because the asymmetries induced by diffusion are an order of magnitude smaller here.

2 The biochemical response circuit

We now consider how the underlying biochemical system might respond to changes in the ECT-2 signal at the cortex.We consider four species: ECT-2 (E), inactive Rho (P), active Rho (ρ), and actomyosin (M), with interactions shown in Fig. 5. The main question we need to answer is the functional form by which inactive Rho and active Rho are exchanged/converted amongst each other. Based on the analysis of [3], we assume the reaction to be auto-catalytic (the forward rate is proportional to active ρ). Based on the data that ECT-2 has a roughly 2:1 A/P ratio, while ρ has a roughly 10:1 ratio, we assume nonlinearity in E as well. Finally, we assume that actomyosin M converts active Rho to inactive Rho via RhoGAP (which colocalizes with actin) [3]. Our total reaction term is therefore,

$$R(P,\rho,E,M) = K_{\mathrm{EP}}E^2\left(\frac{\rho}{G_{\mathrm{PP}}+\rho}\right)P - K_{\mathrm{MP}}M\rho, \tag{4a}$$

which leaves three unknown constants: K_{EP}, K_{MP}, and G_{PP}.

Once we formulate the reaction term converting inactive Rho to active Rho, it is straightforward to formulate the rest of the dynamics. As in [2], we assume that inactive Rho binds from the cytoplasm onto the membrane, where it is converted to active Rho using (4a). Once active, ρ produces myosin. In a system of units where length is in units of the embryo perimeter L, and time is in units of the bound myosin lifetime $1/k_M^{\mathrm{off}}$, the general equations governing the circuit can consequently be written as

$$\partial_t E + \sigma_0\partial_x\left(vE\right) = D_E\partial_x^2 E + K_E^{\mathrm{on}}E_c - K_E^{\mathrm{off}}\left(1+K_{\mathrm{AE}}A\right)E \tag{4b}$$

$$\partial_t P + \sigma_0\partial_x\left(vP\right) = D_P\partial_x^2 P + K_P^{\mathrm{on}}P_c - K_E^{\mathrm{off}}P - R(P,\rho,E,M) \tag{4c}$$

$$\partial_t \rho + \sigma_0\partial_x\left(v\rho\right) = D_\rho\partial_x^2\rho + R(P,\rho,E,M) \tag{4d}$$

$$\partial_t M + \sigma_0\partial_x\left(vM\right) = D_M\partial_x^2 M + K_M^{\mathrm{on}}\left(1+K_{\mathrm{PM}}\frac{\rho}{G_{\mathrm{PM}}+\rho}\right)M_c - M \tag{4e}$$

$$v = \ell^2\partial_x^2 v + \ell\partial_x M \tag{4f}$$

$$E_c = 1-\int_0^1 E(x)\,dx \qquad P_c = 1-\int_0^1 \left(P(x)+\rho(x)\right)\,dx \qquad M_c = 1-\int_0^1 M(x)\,dx \tag{4g}$$

In the velocity equation (4f), the lengthscale ℓ is a hydrodynamic lengthscale (roughly 10 μm), normalized in this unit system by the embryo perimeter [4]. The constant $\sigma_0 \approx 0.026$ is the scale of the active stres induced by myosin, and has been determined elsewhere, along with the form of the stress itself $\sigma_a = M$.

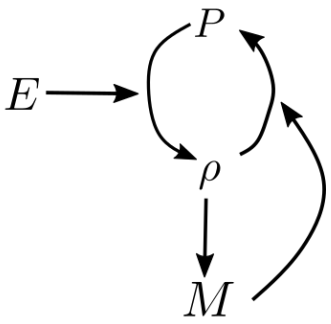

Figure 5: The circuit we consider in this report.

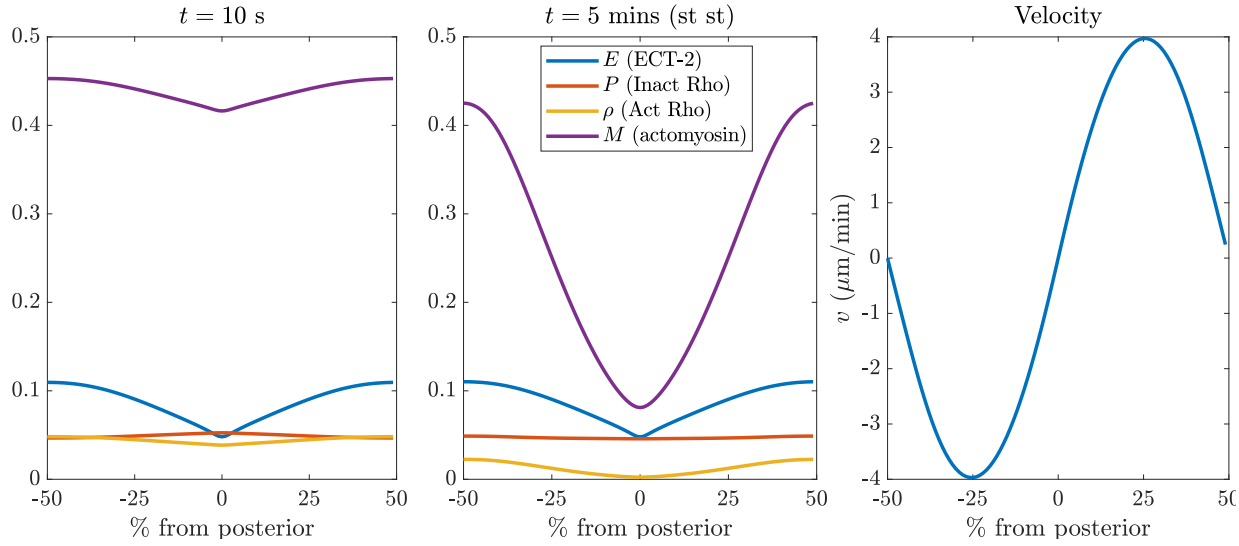

Figure 6: How the AIR-1 signal and ECT-2 profile set the downstream concentrations. Left plot: initially, ECT-2 assumes its asymmetric profile. Middle plot: this sets up a steady state with asymmetric myosin and active Rho. Right plot: velocity at steady state in μm/min.

Discounting the off and on rates, which can be determined directly and from the percentage of protein that is bound at steady state, respectively, there are a total of six unknown constants: K_{EP}, K_{MP}, G_{PP} (in the Rho reaction), and K_{AE}, K_{PM}, and G_{PM} (in the other reactions). Figure **??** tells us that $K_{\mathrm{AE}} \approx 1$. To set the parameters K_{EP}, K_{MP}, and K_{PM}, we look for a regime where roughly 10% of bound Rho is active, and the asymmetry in active Rho is about 10:1. We do this by first specifying G_{PM} and G_{PP}. Far below these constants, the ρ signal is linear, while above them it saturates. We want to operate in the linear regime, and since we expect about 10% of the Rho to be bound to the membrane, we take $G_{\mathrm{PM}} = G_{\mathrm{PP}} = 0.2$. The other parameters are set so that we have a roughly 10:1 asymmetry in myosin and active Rho. The steady state results are shown in Fig. 6.

References

[1] Katrina M Longhini and Michael Glotzer. Aurora a and cortical flows promote polarization and cytokinesis by inducing asymmetric ect-2 accumulation. *Elife*, 11:e83992, 2022.

[2] Ani Michaud, Marcin Leda, Zachary T Swider, Songeun Kim, Jiaye He, Jennifer Landino, Jenna R Valley, Jan Huisken, Andrew B Goryachev, George von Dassow, et al. A versatile cortical pattern-forming circuit based on rho, f-actin, ect2, and rga-3/4. *Journal of Cell Biology*, 221(8):e202203017, 2022.

[3] Jonathan B Michaux, François B Robin, William M McFadden, and Edwin M Munro. Excitable rhoa dynamics drive pulsed contractions in the early c. elegans embryo. *Journal of Cell Biology*, 217(12):4230–4252, 2018.

[4] Arnab Saha, Masatoshi Nishikawa, Martin Behrndt, Carl-Philipp Heisenberg, Frank Jülicher, and Stephan W Grill. Determining physical properties of the cell cortex. *Biophysical journal*, 110(6):1421–1429, 2016.